



# The Equivalence of Dissipation from Gibbs' Entropy Production with Phase-Volume Loss in Ergodic Heat-Conducting Oscillators

Puneet Kumar Patra  
*Advanced Technology Development Center,  
Department of Civil Engineering,  
Indian Institute of Technology, Kharagpur,  
West Bengal 721302, India*

William Graham Hoover\* and Carol Griswold Hoover  
*Ruby Valley Research Institute, Highway Contract 60,  
Box 601, Ruby Valley, Nevada 89833, USA  
\*hooverwilliam@yahoo.com*

Julien Clinton Sprott  
*Department of Physics,  
University of Wisconsin – Madison,  
Wisconsin 53706, USA*

Received November 13, 2015

Gibbs' thermodynamic entropy is given by the logarithm of the phase volume, which itself responds to heat transfer to and from thermal reservoirs. We compare the thermodynamic dissipation described by (i) phase-volume loss with (ii) heat-transfer entropy production. Their equivalence is documented for computer simulations of the response of an ergodic harmonic oscillator to thermostated temperature gradients. In the simulations one or two thermostat variables control the kinetic energy or the kinetic energy and its fluctuation. All of the motion equations are time-reversible. We consider both *strong* and *weak* control variables. *In every case, the time-averaged dissipative loss of phase-space volume coincides with the entropy produced by heat transfer.* Linear-response theory nicely reproduces the small-gradient results obtained by computer simulation. The thermostats considered here are *ergodic* and provide simple dynamical models, some of them with as few as *three* ordinary differential equations, while remaining capable of reproducing Gibbs' canonical phase-space distribution and are precisely consistent with irreversible thermodynamics.

*Keywords:* Ergodicity; algorithms; entropy production; dissipation.

## 1. Introduction

We discuss the time-reversibility and thermodynamic dissipation of several harmonic-oscillator models, all of them *extensions* of the thermostated canonical-ensemble dynamics pioneered by Shuichi Nosé [1984a, 1984b]. All the resulting extended

models [Hoover, 1985, 1997; Martyna *et al.*, 1992; Ju & Bulgac, 1993; Hoover & Holian, 1996; Hoover *et al.*, 2015a; Bulgac & Kusnezov, 1990; Kusnezov *et al.*, 1990; Hoover *et al.*, 2015b; Hoover *et al.*, 2016; Hoover *et al.*, 2015c] studied here are chaotic and ergodic. They generate phase-space distributions

---

\*Author for correspondence

matching Gibbs' canonical distribution, Gaussian in the oscillator coordinate  $q$  and momentum  $p$  with halfwidths of order  $\sqrt{T}$  corresponding to a heat reservoir with kinetic temperature  $T$ .

Our *nonequilibrium* extensions of these equilibrium models result when the thermostat temperature has a spatial gradient with  $T = T(q)$ . All such nonequilibrium models discussed here generate time-averaged heat flows obeying the Second Law of Thermodynamics. All these nonequilibrium models generate *fractal* rather than smooth phase-space distributions. The fractals' time dependence chronicles the penetration of the fractal character to smaller and smaller length scales with passing time, and is fully consistent with Gibbs' phase-volume definition of entropy.

We begin with a brief discussion of time reversibility and ergodicity in Sec. 2. Section 3 provides a historical sketch of time-reversible thermostat models from Nosé's work to the present. Section 4 illustrates the time-reversibility of the models in nonequilibrium stationary flows and demonstrates the consistency of all the thermostat models with Gibbs' statistical thermodynamics. Section 5 illustrates the consistency of these steady flows with Green and Kubo's treatment of near-equilibrium linear-response theory. We consider the details of the linear-response approach for two models [Hoover & Holian, 1996; Hoover et al., 2015b]. Our summary and historical perspective in Sec. 6 includes our main conclusion from this work: useful computational thermostats can be and should be chosen so that the thermodynamic dissipation away from equilibrium is consistent with the Second Law of Thermodynamics where the entropy corresponds to Gibbs' phase-volume definition. We relate this finding to the history of understanding microscopic systems through the computational study of small-system dynamics.

## 2. Time-Reversible Ergodicity at and Away from Equilibrium

Thirty years ago, Nosé and Hoover developed two new mechanics formally consistent with Gibbs' canonical ensemble [Nosé, 1984a, 1984b; Hoover, 1985, 1997]. These modern mechanics share two fundamental characteristics of their Hamiltonian ancestor, being both deterministic and *time-reversible*. Any sequence of successive frames of a Nosé or Nosé-Hoover movie played "backward", with the frames in reversed order, shows a reversed

motion described by exactly the same motion equations but with reversed velocities. Hamiltonian mechanics shares this same time-reversibility property.

The harmonic oscillator provides the simplest example of reversibility. If we choose a one-dimensional harmonic oscillator with unit mass and spring constant then any "forward" orbit (with  $-\tau < t < +\tau$ ) can be paired with a time-reversed backward twin with the reversal occurring at time  $t = 0$ . For instance:

$$\begin{aligned} \{q = \pm \sin(t); p = \pm \cos(t)\} \\ \leftrightarrow \{q = \mp \sin(t); p = \mp \cos(t)\}. \end{aligned}$$

Both orbits satisfy Hamilton's equations:  $\{\dot{q} = +p; \dot{p} = -q\}$ . In this simplest case the reversed version is also a mirror image of the original, with both  $q$  and  $p$  changed in sign. In both cases, forward and backward, time *increases*. This corresponds to a positive timestep  $dt > 0$  in a numerical simulation. We distinguish this *physical* version of "time-reversibility" with  $+p \rightarrow -p$  from its *mathematical* cousin where  $dt$  changes sign while  $q$  and  $p$  do not.

Nosé sought out a dynamics which would explore the  $(q, p)$  phase space with a probability density approaching Gibbs' canonical distribution,  $f(q, p) \propto e^{-\mathcal{H}(q,p)/kT}$ . Both the Nosé and the simpler Nosé-Hoover thermostat algorithms lacked the ergodicity required to reproduce all of Gibbs' canonical distribution for the prototypical one-dimensional harmonic oscillator [Hoover, 1985].

About a decade later, three more-complex algorithms, *doubly-thermostated* with four motion equations rather than singly-thermostated with three, were developed. All three have been shown to provide ergodicity for the oscillator [Martyna et al., 1992; Ju & Bulgac, 1993; Hoover & Holian, 1996; Hoover et al., 2015a]. How to demonstrate this ergodicity? First of all, ergodic motion equations necessarily satisfy the *stationary* version of Liouville's continuity equation:

$$\left(\frac{\partial f}{\partial t}\right) = -\nabla_r \cdot (fv) \equiv 0.$$

Abbreviate the Nosé-Hoover motion equations for an oscillator by introducing a generalized velocity  $v$  for the three-dimensional flow:

$$\begin{aligned} v = \dot{r} = (\dot{q}, \dot{p}, \dot{\zeta}) \\ \leftarrow \left\{ \dot{q} = +p; \dot{p} = -q - \zeta p; \dot{\zeta} = \left(\frac{p^2}{T}\right) - 1 \right\} \quad \text{[NH]}, \end{aligned}$$

where the stationary distribution  $f$  is proportional to  $e^{-q^2/2T}e^{-p^2/2T}e^{-\zeta^2/2}$ . The four nonvanishing contributions to  $(\partial f/\partial t)$  are:

$$\begin{aligned} -\dot{q}\left(\frac{\partial f}{\partial q}\right) &= p\left(\frac{q}{T}\right)f; \\ -\dot{p}\left(\frac{\partial f}{\partial p}\right) &= (-q - \zeta p)\left(\frac{p}{T}\right)f; \\ -\dot{\zeta}\left(\frac{\partial f}{\partial \zeta}\right) &= \left[\left(\frac{p^2}{T}\right) - 1\right](\zeta)f; \\ -f\left(\frac{\partial \dot{p}}{\partial p}\right) &= f\zeta. \end{aligned}$$

These four terms sum up to zero, showing that the motion equations are consistent with the assumed Gaussian distribution. The Nosé–Hoover equations are *not* ergodic so that the vanishing of  $(\partial f/\partial t)$  is not *sufficient* for ergodicity. In fact, numerical work shows that only a bit less than 6% of the Gaussian oscillator measure is mixing and chaotic. The remaining 94% is made up of regular tori, showing that the Nosé–Hoover distribution is not ergodic. See Fig. 1 for a cross-sectional view of the Nosé–Hoover oscillator's chaotic sea. We use the term “chaotic” in the usual sense here, to indicate that the maximum Lyapunov exponent has a long-time positive average value. Numerical methods for measuring Lyapunov exponents so as to characterize chaos make up a vast literature readily accessible through Wikipedia.

Ergodic motion equations must necessarily reproduce the canonical moments of the Maxwell–Boltzmann velocity distribution. With  $mkT$  chosen equal to unity to set the temperature scale, the values appropriate for Cartesian coordinates,

$$\langle p^{2,4,6,\dots} \rangle_{MB} = 1, 3, 15, \dots$$

can readily be verified from numerical simulations. But distributions which are “almost” ergodic (for some specific aesthetic examples see Figs. 2–4 in [Hoover *et al.*, 2015c]) can exhibit deviations so small as to be masked by thermal fluctuations.

Two better checks of ergodicity have been implemented. Cross-sections (such as the  $(q, p, 0)$  points shown in Fig. 1), where  $\zeta = 0$  or where  $\zeta = \xi = 0$  if two thermostat variables are used can be inspected visually for the tell-tale holes indicating regular toroidal solutions within the chaotic sea.

Additionally, the mean value of the largest Lyapunov exponent  $\lambda_1$  (the long-time averaged rate of

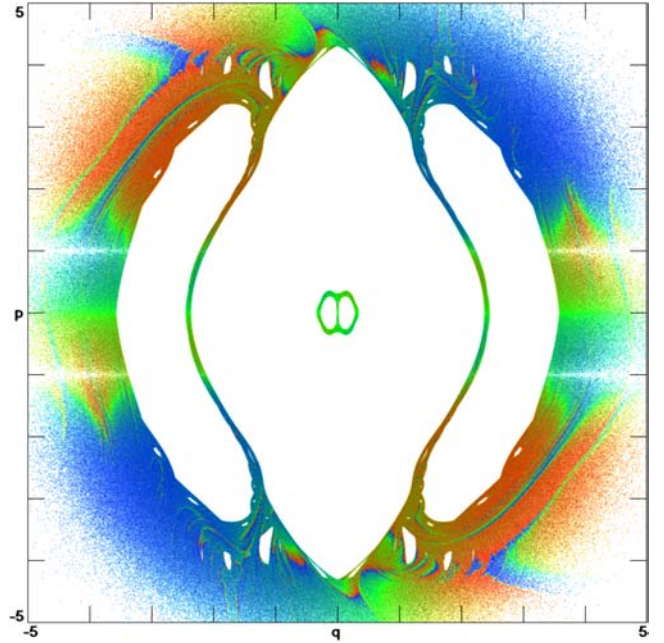


Fig. 1. Penetrations of the  $(q, p, 0)$  plane for the chaotic Nosé–Hoover oscillator with initial condition  $(0, 5, 0)$ , using points from an adaptive fourth-order Runge–Kutta integration with a timestep  $dt \simeq 0.001$ . Red and blue correspond to the most positive and most negative Lyapunov exponents. Notice the lack of symmetry about the horizontal axis despite the time-reversibility of the equations of motion, showing that the Lyapunov exponents' dependence on past history differs from their relation to the unforeseeable future. This cross-section of the chaotic sea corresponds to about 6% of the Nosé–Hoover oscillator's Gaussian measure. Note the mirror-image inversion symmetry.

separation of two nearby trajectories, positive for chaos and zero for tori) can be estimated for simulations using millions or billions of randomly chosen initial conditions. For an *ergodic* system the results cluster around a unique positive long-time average,  $\langle \lambda_1(t) \rangle \simeq \lambda_1$ . For a toroidal system the averaged results instead cluster about zero.

The three criteria (moments, tell-tale holes, Lyapunov exponent) have been applied to the thermostats described in the following section leading to the conclusion that many different one-thermostat and two-thermostat systems *are* ergodic. Let us detail four such systems next.

### 3. Deterministic Time-Reversible Thermostats (1984–2015)

As recently as early 2015 it was thought that four or more ordinary differential equations were required for oscillator ergodicity. [Hoover *et al.*, 2015a] deals with techniques for demonstrating ergodicity as

applied to the Martyna–Klein–Tuckerman [1992], Ju–Bulgac [1993], and Hoover–Holian [1996] thermostated oscillators. For a more comprehensive treatment see [Bulgac & Kusnezov, 1990; Kusnezov *et al.*, 1990]. The three thermostat types, MKT, JB, and HH, produce chaotic dynamics ( $\dot{q}, \dot{p}, \dot{\zeta}, \dot{\xi}$ ) which pass visual ergodicity tests. All three of them also closely reproduce the Cartesian velocity moments  $\langle p^{2,4,6} \rangle$  characterizing the equilibrium Maxwell–Boltzmann distribution. Let us begin by reviewing the structure of these three thermostat types.

### 3.1. The Martyna–Klein–Tuckerman “Chain” thermostat (1992)

The Martyna–Klein–Tuckerman thermostat uses two control variables,  $\zeta$  and  $\xi$ , with  $\zeta$  controlling  $\langle p^2 \rangle$  and  $\xi$  controlling  $\langle \zeta^2 \rangle$ :

$$\left\{ \begin{aligned} \dot{q} &= p; \dot{p} = -q - \zeta p; \\ \dot{\zeta} &= \left( \frac{p^2}{T} \right) - 1 - \xi \zeta; \dot{\xi} = \zeta^2 - 1 \end{aligned} \right\} \quad \text{[MKT].}$$

The steady-state distribution corresponding to these oscillator motion equations is an extension of Gibbs’ canonical one:

$$\begin{aligned} f_{\text{MKT}}(q, p, \zeta, \xi) &\propto e^{-q^2/2T} e^{-p^2/2T} e^{-\zeta^2/2} e^{-\xi^2/2} \rightarrow \left( \frac{\partial f}{\partial t} \right) \\ &= -\nabla_r \cdot (fv) \\ &\equiv 0 \quad \text{where } v = \dot{r} \equiv (\dot{q}, \dot{p}, \dot{\zeta}, \dot{\xi}). \end{aligned}$$

The *stationarity* test from the continuity equation,  $(\partial f/\partial t) = 0$ , provides a necessary, but not necessarily sufficient, condition that *any* set of motion equations must satisfy for ergodicity. Martyna *et al.* [1992] emphasized that any number of additional control variables can be added to form a “chain” of thermostats.

### 3.2. The Ju–Bulgac cubic thermostat (1993)

The Ju–Bulgac thermostat [1993] likewise uses two control variables but includes *cubic* dependences following the observation of Bauer, Bulgac, and Kusnezov that cubic terms enhance chaos and ergodicity [Ju & Bulgac, 1993; Bulgac & Kusnezov, 1990; Kusnezov *et al.*, 1990]:

$$\left\{ \begin{aligned} \dot{q} &= p; \dot{p} = -q - \zeta^3 p - \xi \left( \frac{p^3}{T} \right); \dot{\zeta} = \left( \frac{p^2}{T} \right) - 1; \\ \dot{\xi} &= \left( \frac{p^4}{T^2} \right) - 3 \left( \frac{p^2}{T} \right) \end{aligned} \right\} \quad \text{[JB].}$$

The steady-state distribution here is Gaussian in  $\zeta^2$  rather than  $\zeta$ :

$$\begin{aligned} f_{\text{JB}}(q, p, \zeta, \xi) &\propto e^{-q^2/2T} e^{-p^2/2T} e^{-\zeta^4/4} e^{-\xi^2/2} \\ &\rightarrow \left( \frac{\partial f}{\partial t} \right) \equiv 0. \end{aligned}$$

At unit temperature  $T = 1$  the rms rate  $\sqrt{\langle \dot{p}^2 \rangle}$  at which the Ju–Bulgac momentum moves through phase space is about three times faster than that of the simpler Martyna–Klein–Tuckerman momentum:

$$\begin{aligned} &\sqrt{\langle q^2 + p^2 \zeta^6 + p^6 \xi^2 \rangle} \\ &\simeq \sqrt{18.028} \text{ versus } \sqrt{\langle q^2 + p^2 \zeta^2 \rangle} = \sqrt{2}. \end{aligned}$$

From the numerical standpoint cubic thermostat variables enhance chaos and mixing without incurring the considerable stiffness associated with quintic controls.

### 3.3. The Hoover–Holian thermostat (1996)

Like the two preceding, the Hoover–Holian thermostat [1996] uses two control variables. The first one is allocated to fixing the oscillator temperature  $\zeta \rightarrow \langle p^2 \rangle$  while the second fixes the fluctuation of the temperature  $\xi \rightarrow \langle p^4 \rangle$ :

$$\left\{ \begin{aligned} \dot{q} &= p; \dot{p} = -q - \zeta p - \xi \left( \frac{p^3}{T} \right); \\ \dot{\zeta} &= \left( \frac{p^2}{T} \right) - 1; \dot{\xi} = \left( \frac{p^4}{T^2} \right) - 3 \left( \frac{p^2}{T} \right) \end{aligned} \right\} \quad \text{[HH].}$$

At unit temperature the rms rate at which the Hoover–Holian momentum moves,

$$\sqrt{\langle q^2 + p^2 \zeta^2 + \xi^2 p^6 \rangle} = \sqrt{17},$$

is nearly the same as the Ju–Bulgac speed. The Hoover–Holian thermostat variables  $\zeta$  and  $\xi$  exert what we term “strong” control of the temperature and its fluctuation, in that long-time averages of the thermostat motion equations constrain moments proportional to the kinetic energy and its

fluctuation:

$$\langle \dot{\zeta} \rangle = 0 \rightarrow \left\langle \left( \frac{p^2}{T} \right) \right\rangle \equiv 1;$$

$$\langle \dot{\xi} \rangle = 0 \rightarrow \left\langle \left( \frac{p^4}{T^2} \right) \right\rangle \equiv \left\langle 3 \left( \frac{p^2}{T} \right) \right\rangle.$$

These strong constraints can be applied equally well in nonequilibrium situations. Nonequilibrium applications of the MKT thermostat typically lead to nonzero correlated values of the thermostat variables,  $\langle \zeta \xi \rangle$  so that the definition of the kinetic temperature  $\langle (p^2/T) \rangle \equiv 1$  is violated.

At equilibrium the steady-state distribution corresponding to the HH motion equations is exactly the same as the Martyna–Klein–Tuckerman four-dimensional Gaussian:

$$f_{\text{HH}}(q, p, \zeta, \xi) = f_{\text{MKT}}(q, p, \zeta, \xi)$$

$$\propto e^{-q^2/2T} e^{-p^2/2T} e^{-\zeta^2/2} e^{-\xi^2/2}$$

$$\rightarrow \left( \frac{\partial f}{\partial t} \right) \equiv 0.$$

### 3.4. The ergodic single-thermostat 0532 Model (2015)

Very recently [Hoover *et al.*, 2015b; Hoover *et al.*, 2016; Hoover *et al.*, 2015c] a variety, both novel and wide, of *singly*-thermostated ergodic algorithms has been developed and applied to the one-dimensional harmonic oscillator. The simplest of them, the “0532 Model”, consists of only three ordinary differential equations for the oscillator coordinate  $q$ , velocity  $p$ , and friction coefficient  $\zeta$  at a thermostat temperature  $T$ :

$$\dot{q} = p;$$

$$\dot{p} = -q - \zeta \left[ 0.05p + 0.32 \left( \frac{p^3}{T} \right) \right];$$

$$\dot{\zeta} = 0.05 \left[ \left( \frac{p^2}{T} \right) - 1 \right] + 0.32 \left[ \left( \frac{p^4}{T^2} \right) - 3 \left( \frac{p^2}{T} \right) \right];$$

[0532 Model].

We term this simultaneous control of the second and fourth moments,  $\langle p^2 \text{ and } 4 \rangle$ , “weak” because a linear combination of the moments is controlled rather than enforcing the separate control of *both* moments, as in the earlier work in [Martyna *et al.*, 1992; Ju & Bulgac, 1993; Hoover & Holian, 1996; Hoover *et al.*, 2015a; Bulgac & Kusnezov, 1990].

Numerical solutions of the 0532 oscillator model indicate that it *is* ergodic and corresponds to Gibbs' canonical ensemble multiplied by a Gaussian distribution for the thermostat control variable  $\zeta$ :

$$f_{0532}(q, p, \zeta, \xi) = \propto e^{-q^2/2T} e^{-p^2/2T} e^{-\zeta^2/2}$$

$$\rightarrow \left( \frac{\partial f}{\partial t} \right) \equiv 0.$$

Because the 0532 Model motion occurs in just three dimensions rather than four, it is well-suited to analysis. This model, like its three predecessors in this section, is time-reversible, even in the nonequilibrium case where the temperature varies in space,  $T = T(q)$ . Let us review the reversibility property in that specific *nonequilibrium* case.

### 4. Time-Reversibility Away from Equilibrium — 0532 Model

At equilibrium the forward and backward trajectories for canonical oscillators, using any of the four ergodic sets of motion equations, are qualitatively much the same. No holes in the cross-sections, good values for the even velocity moments, long-time averaged Lyapunov exponent being the same for any initial condition. In short — deterministic, time-reversible, ergodic.

*Away from* equilibrium, thermodynamic dissipation can be investigated, still time-reversibly, by adding a localized temperature gradient  $(dT/dq) = [\epsilon/\cosh^2(q)]$  enabling heat transfer through a nonzero average current  $(p^3/2)$ :

$$1 - \epsilon < T < 1 + \epsilon = T(q) = 1 + \epsilon \tanh(q)$$

$$\rightarrow \left\langle \left( \frac{p^3}{2} \right) \right\rangle < 0 \leftrightarrow \left\langle \left( \frac{\dot{S}}{k} \right) \right\rangle < 0.$$

Here  $\epsilon$  is the maximum value of the temperature gradient,  $T'(0)$ . The negative entropy change, causing the phase volume to shrink onto a strange attractor is due to the net heat loss *from* the oscillator *to* the coordinate-dependent 0532 thermostat temperature  $T(q)$ . From the standpoint of steady-state irreversible thermodynamics the overall heat loss is offset by an internal “entropy production” so that the *net* change of oscillator “entropy” vanishes. We remind the reader that Gibbs' entropy is actually minus infinity for fractal attractors so that the irreversible-thermodynamics concept of nonequilibrium entropy is problematic. The artificial entropy change could also be viewed as the

result of ongoing coarse-graining (which would artificially increase Gibbs' entropy) at the level of the computational roundoff error (in the 16th or 17th digit).

The temperature gradient destroys the “global (overall) reversibility” of the motion equations. Although in principle reversible everywhere, the chaotic instability of the dynamics, evidenced by a positive Lyapunov exponent, makes this “irreversibility” possible. This irreversibility is evidenced by a Lyapunov spectrum with a *negative* sum so that the long-time averaged distribution is a fractal strange attractor with a reduced information dimension rather than a smooth three-dimensional Gibbsian distribution.

Among the thermostats we have considered only the Nosé–Hoover equations show that a fractal attractor is *not* inevitable. In the Nosé–Hoover case, a majority of initial conditions give rise to phase-space tori, orbits with no long-time tendency toward dissipation. All of the ergodic thermostats invariably produce small-gradient dissipation rather than tori so that their orbits exhibit what we call “global irreversibility”.

The equilibrium ( $\epsilon = 0$  and unit temperature  $T = 1$ ) Lyapunov spectrum for the 0532 Model,

$\{+0.144, 0, -0.144\}$  sums to zero corresponding to the three-dimensional Gaussian distribution,  $f \propto e^{-q^2/2}e^{-p^2/2}e^{-\zeta^2/2}$ . The time-averaged growth rates of infinitesimal one-, two-, and three-dimensional phase-space volumes are given by

$$\{\lambda_1, \lambda_1 + \lambda_2, \lambda_1 + \lambda_2 + \lambda_3\}.$$

In the nonequilibrium case with  $\epsilon = 0.50$  the time-averaged spectrum becomes asymmetric,  $\{+0.1135, 0, -0.1454\}$ , corresponding to the time-averaged growth of a length or an area in phase space  $\simeq e^{+0.1135t}$  but to *shrinkage* of an infinitesimal three-dimensional phase-volume  $\otimes$ :

$$\left(\frac{\dot{\otimes}}{\otimes}\right) = 0.1135 - 0.1454 = -0.0319$$

$$\rightarrow D_{KY} = 2 + \left(\frac{0.1135}{0.1454}\right) = 2.78.$$

Kaplan and Yorke's linear interpolation predicts a strange-attractor dimension of 2.78. Cross-sections of the equilibrium and nonequilibrium 0532 dynamics are shown in Fig. 2. Just as at equilibrium, the nonequilibrium strange-attractor's motion equations are time-reversible. Any forward-in-time sequence  $\{+q, +p, +\zeta\}$  corresponds to a

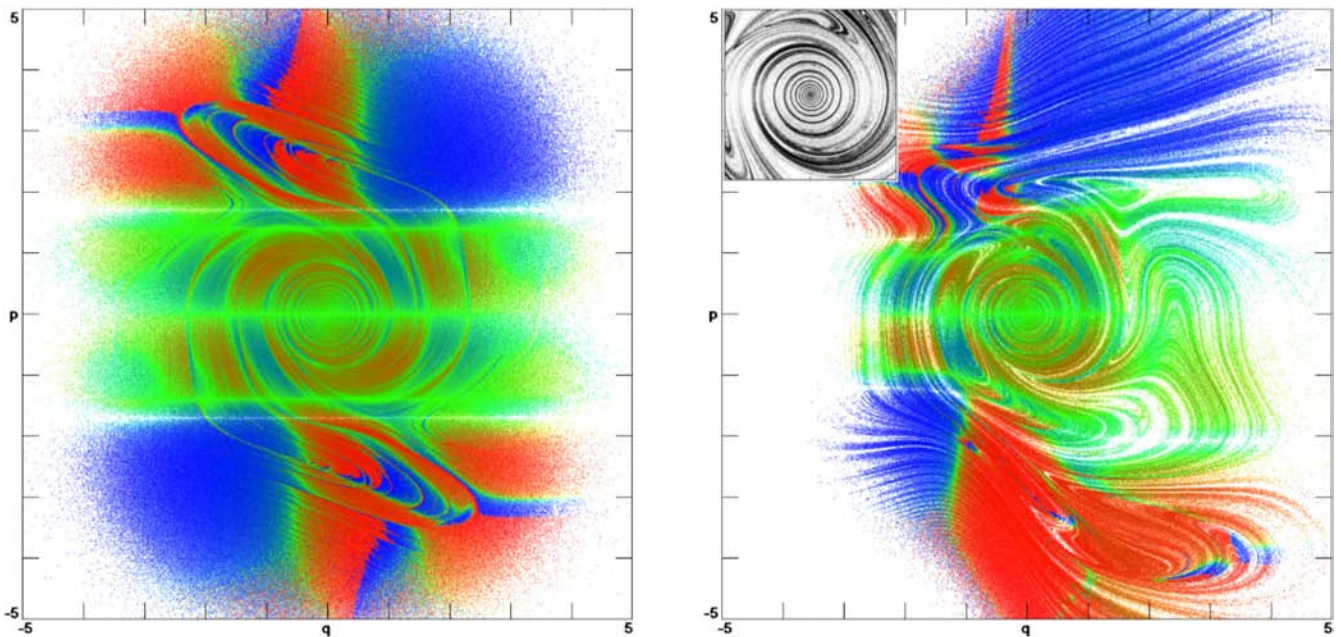


Fig. 2. Penetrations of the  $(q, p, 0)$  plane for the chaotic and ergodic 0532 Model using adaptive fourth-order Runge–Kutta integration with a timestep  $dt \simeq 0.001$ . The red and blue points correspond to maximum and minimum values of the local Lyapunov exponent. The equilibrium  $\zeta = 0$  cross-section at the left shows inversion symmetry, corresponding to viewing the oscillator in a mirror. The lack of symmetry about the horizontal  $p = 0$  axis shows that the exponents depend upon the past rather than the future. The nonequilibrium section ( $\epsilon = 0.50$ ) shown to the right displays no symmetry and is multifractal. The black-and-white inset shows the cross-sectional density in the  $2 \times 2$  central region of the phase-plane section.

twin sequence  $\{+q, -p, -\zeta\}$  with the order of  $(q, p, \zeta)$  points reversed. *Locally* this reversed sequence satisfies the same equations of motion with errors of order  $(dt^5/120)$  for fourth-order Runge–Kutta integration [Hoover & Hoover, 2015]. But any attempt to *generate* such a reversed sequence numerically fails because the Lyapunov spectrum of the reversed sequence would correspond to  $\{+0.1454, 0, -0.1135\}$ . The positive exponent sum indicates an unstable *repellor* with a *diverging* phase volume,  $(\dot{\otimes}/\otimes) \simeq +0.0319$ . Any attempt to follow the repellor numerically will instead seek out the nearby attractor (both are still ergodic, at least if  $\epsilon$  is small) which, though chaotic with  $\lambda_1 = \langle \lambda_1(t) \rangle > 0$ , is less so than the repellor. The repellor properties *can* (only) be observed by the expedient of *storing* and reversing a trajectory. The cross-section associated with a stored ten-billion-point attractor trajectory is illustrated in Fig. 3. Note the lack of both  $\pm p$  and inversion symmetry in the sign of the local Lyapunov exponent,  $\lambda_1(t)$ .

This instructive problem illustrates two general principles: (i) the phase-volume of the steady-state

attractor is zero and singular everywhere *despite the time-reversibility of the motion equations*; (ii) a typical three-dimensional phase-volume  $\otimes$  first expands or contracts according to the sign of  $\zeta \equiv \sum \lambda$ . Presently with  $\langle \dot{\otimes}/\otimes \rangle \simeq -0.0139$  the distorted volume leaves the vicinity of the (ergodic) fractal repellor and then shrinks in order to join its mirror-image (and likewise ergodic) fractal attractor with a perpetually decreasing phase-volume of order  $e^{-0.0139t}$ . Both these features correspond to the paucity of nonequilibrium states and to the irreversibility described by the Second Law of Thermodynamics.

There is more. Consider two additional equally-significant observations. First, the comoving shrinkage rate in phase space corresponds precisely and instantaneously to the loss of Gibbs' entropy for the system. To illustrate consider the 0532 Model,

$$\dot{q} = p; \quad \dot{p} = -q - \zeta \left[ 0.05p + 0.32 \left( \frac{p^3}{T} \right) \right];$$

$$\dot{\zeta} = 0.05 \left[ \left( \frac{p^2}{T} \right) - 1 \right] + 0.32 \left[ \left( \frac{p^4}{T^2} \right) - 3 \left( \frac{p^2}{T} \right) \right].$$

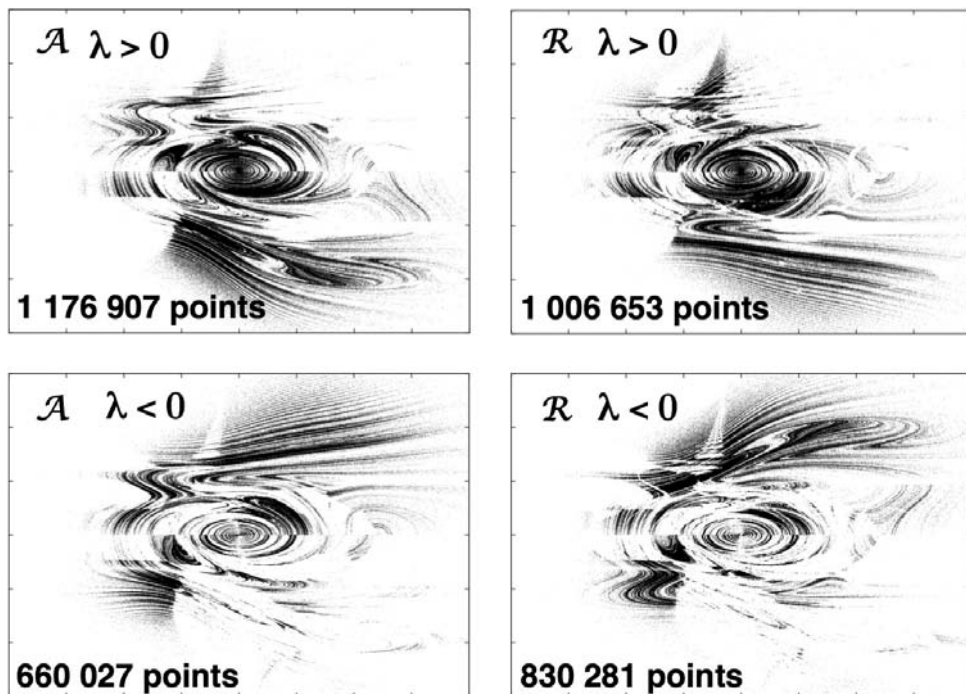


Fig. 3. Penetrations of the  $(q, p, 0)$  plane for the chaotic and ergodic 0532 Model using a ten-billion-point attractor reference trajectory (denoted A) and classic fourth-order Runge–Kutta integration with a timestep  $dt = 0.001$  for the satellite trajectory. This chaotic trajectory crosses the  $\zeta = 0$  plane 1836 934 times. The signs of the largest Lyapunov exponent at each crossing are indicated for both the attractor and the repellor (denoted R). By plotting the positive and negative points separately, the lack of any symmetry is clear. The repellor points are identical to those of the attractor but are traced out in the opposite direction. For both the attractor and the repellor the separation of the reference and satellite trajectories is  $\sqrt{(q_s - q_r)^2 + (p_s - p_r)^2 + (\zeta_s - \zeta_r)^2} = 0.000001$ . The  $p(q)$  region shown is  $|q| < 4$ ;  $|p| < 6$ .

$$\begin{aligned} \left(\frac{\dot{S}}{k}\right) &= \left(\frac{\dot{\otimes}}{\otimes}\right) \equiv \left(\frac{\partial \dot{q}}{\partial q}\right) + \left(\frac{\partial \dot{p}}{\partial p}\right) + \left(\frac{\partial \dot{\zeta}}{\partial \zeta}\right) \\ &= 0 - \zeta \left[0.05 + 0.96 \left(\frac{p^2}{T}\right)\right] + 0. \end{aligned}$$

Second, this loss rate also corresponds precisely, *when time-averaged*, to the kinetic energy (or heat  $Q$ ) extracted by the thermostat forces, divided by the thermostat temperature  $T$ :

$$\begin{aligned} \left\langle \left(\frac{\dot{Q}}{T}\right) \right\rangle &= - \left\langle \zeta \left[0.05 \left(\frac{p^2}{T}\right) + 0.32 \left(\frac{p^4}{T^2}\right)\right] \right\rangle \\ &= \left\langle \left(\frac{\dot{S}}{k}\right) \right\rangle. \end{aligned}$$

The time-averaged value  $\langle \zeta [0.05 + 0.96(p^2/T)] \rangle$ , follows from the time-averaged evolution equation for the squared thermostat variable ( $\zeta^2/2$ ):

$$\begin{aligned} \left\langle \zeta \dot{\zeta} = 0 = 0.05\zeta \left[\left(\frac{p^2}{T}\right) - 1\right] \right. \\ \left. + 0.32\zeta \left[\left(\frac{p^4}{T^2}\right) - 3\left(\frac{p^2}{T}\right)\right] \right\rangle. \end{aligned}$$

The time-averaged phase-volume loss, equivalent to the dissipation seen in the heat  $Q$  lost to thermal reservoirs divided by the reservoir temperature  $T$ ,

$$\left\langle \left(\frac{\dot{Q}}{T}\right) \right\rangle = \left\langle k \left(\frac{\dot{\otimes}}{\otimes}\right) \right\rangle = \langle \dot{S} \rangle,$$

holds generally for *all* the thermostat models discussed here. This identity holds even for the Nosé–Hoover model, which is not ergodic. It holds for other power laws. Suppose for instance that the thermostat force is proportional to odd powers of  $\zeta$  and  $p$ :

$$-A_{mn}\zeta^{2m+1} \left(\frac{p^{2n+1}}{T^n}\right)$$

so that the equilibrium distribution is proportional to

$$f \propto e^{-p^2/2T} e^{-\zeta^{2m+2}/(2m+2)}.$$

Gibbs’ phase-space dissipation, from  $-(\partial \dot{p}/\partial p)$  gives a contribution to the system entropy:

$$\left(\frac{\dot{S}}{k}\right) = -(2n+1)A_{mn}\zeta^{2m+1} \left(\frac{p^{2n}}{T^n}\right).$$

The entropy change from the contribution of the same dissipative term to heat transfer is:

$$\left(\frac{\dot{Q}}{T}\right) = -A_{mn}\zeta^{2m+1} \left(\frac{p^{2n+2}}{T^{n+1}}\right).$$

A look at the equation of motion for the friction coefficient, multiplied by  $\zeta^{2m+1}$  and time averaged shows that  $(\dot{S}/k)$  and  $(\dot{Q}/T)$  are equivalent:

$$\begin{aligned} \langle \zeta^{2m+1} \dot{\zeta} \rangle &= \left\langle \zeta^{2m+1} A_{mn} \left[ \left(\frac{p^{2n+2}}{T^{n+1}}\right) - (2n+1) \left(\frac{p^{2n}}{T^n}\right) \right] \right\rangle \\ &= 0. \end{aligned}$$

This is a consequence of the vanishing of the long-time averaged value of a bounded quantity, in this case  $(d/dt)[\zeta^{2m+2}/(2m+2)]$ . Generalized models, like the 0532 Model, can use two or more power-law contributions to thermostat forces. This equivalence of Gibbs’ entropy production with that from irreversible thermodynamics points the way forward toward consistent theories of nonequilibrium steady states either near to or far from equilibrium.

In the past it has been pointed out that it *is* possible to develop thermostats for which the phase-volume and heat-transfer rates are *not* closely related [Daems & Nicolis, 1999; van Beijeren & Dorfman, 2000; Cohen & Rondoni, 1998]. This potential loss of a family relationship recalls Tolstoy’s thought: “All happy families are alike; each unhappy family is unhappy in its own way.” We emphasize here that the close relationship linking phase volume to thermodynamics is to be celebrated rather than avoided.

We note that our dimensionless friction coefficients *could* be multiplied by relaxation times or by powers of the temperature, changing their units. We have carefully chosen the forms used here in order to guarantee the consistency of the motion equations with both Gibbs’ canonical distribution and with thermodynamics. Dimensionless friction coefficients seem to us the simplest approach to thermodynamic consistency.

In the 1950s, Green and Kubo showed that their “linear-response” theory expresses nonequilibrium transport coefficients in terms of equilibrium correlation functions. This same theory can be applied to the various thermostats we have described. Next we illustrate this idea for two examples, the doubly-thermostated Hoover–Holian thermostat and the singly-thermostated 0532 Model.

## 5. Linear Response Theory with a Temperature Gradient

We have celebrated the equivalence of two measures of dissipation, phase-volume loss and Gibbs' entropy production when any one of our five thermostat models (NH, MKT, JB, HH, 0532) is time averaged. This equivalence guarantees their usefulness in simulations consistent with dynamical equivalents of the canonical ensemble. Green-Kubo linear-response theory is a perturbation theory based on Gibbs' ensembles. Typically the energy is modified by a perturbation, giving rise to a nonequilibrium flux. In our case, both the energy and the temperature are modified by introducing a temperature profile along with a stabilizing frictional force. Let us demonstrate their theory's usefulness for the Hoover-Holian ( $q, p, \zeta, \xi$ ) and the 0532 Model ( $q, p, \zeta$ ) oscillators as two concrete examples.

### 5.1. Hoover-Holian oscillator with temperature gradient

We begin with the extended canonical distribution for the oscillator with energy  $E$  and at a temperature  $T$  of unity:

$$\begin{aligned} f(q, p, \zeta, \xi)_{\text{HH}} &\propto e^{-\mathcal{H}(q,p)/kT} e^{-\zeta^2/2} e^{-\xi^2/2} \\ &= e^{-q^2/2T} e^{-p^2/2T} e^{-\zeta^2/2} e^{-\xi^2/2}. \end{aligned}$$

Adding a temperature perturbation,

$$T = 1 \rightarrow T = 1 + \Delta T = 1 + \epsilon \tanh(q),$$

we wish to compute the responding current,  $\langle p^3/2 \rangle$  as a function of time.

The simplest form of the Hoover-Holian motion equations is:

$$\left\{ \begin{aligned} \dot{q} &= p; \dot{p} = -q - \zeta p - \xi \left( \frac{p^3}{T} \right); \dot{\zeta} = \left( \frac{p^2}{T} \right) - 1; \\ \dot{\xi} &= \left( \frac{p^4}{T^2} \right) - 3 \left( \frac{p^2}{T} \right) \end{aligned} \right\} \quad [\text{HH}].$$

The time-dependent change of the canonical weight  $e^{-\Delta(E/kT)}$  can be linearized in the thermal perturbation  $\epsilon$  with the result:

$$\begin{aligned} \left( \frac{f_{\text{neq}}}{f_{\text{eq}}} \right) &= 1 + \int_0^t [\epsilon \tanh(q)]_0 \\ &\times \left[ -\zeta p^2 - \xi \left( \frac{p^4}{T^2} \right) \right]_{t'} dt'. \end{aligned}$$

We can use this *nonequilibrium* perturbation to compute the current  $\langle p^3/2 \rangle$  at time  $t$  from the *equilibrium* correlation function (which depends only on the time difference  $t'$ ):

$$\begin{aligned} \left\langle \left( \frac{p^3}{2} \right) \right\rangle_{\text{neq}} &= \int_0^t \left\langle [\epsilon \tanh(q)]_0 \right. \\ &\times \left. \left[ -\zeta p^2 - \xi \left( \frac{p^4}{T^2} \right) \right]_0 \left( \frac{p^3}{2} \right)_{t'} \right\rangle_{\text{eq}} dt'. \end{aligned}$$

A highly-accurate equilibrium calculation can be based on the fact that the four-dimensional equilibrium measure is ergodic, a Gaussian probability density known in advance. To compute averages we begin with a grid of  $[100 \times 100 \times 100 \times 100]$  equiprobable points and use these as the initial conditions for computing both the nonequilibrium current and the equilibrium correlation function. The excellent agreement shown in Fig. 4 confirms the analysis showing that both the equilibrium distribution function and its linear perturbation are well suited to numerical exploration. The figure compares the linear-response expression for the current to that actually measured with nonequilibrium molecular dynamics at the relatively small field strength  $\epsilon = 0.10$ . We conclude that simple linear-response theory is a fringe benefit of our deterministic ergodic thermostat models.

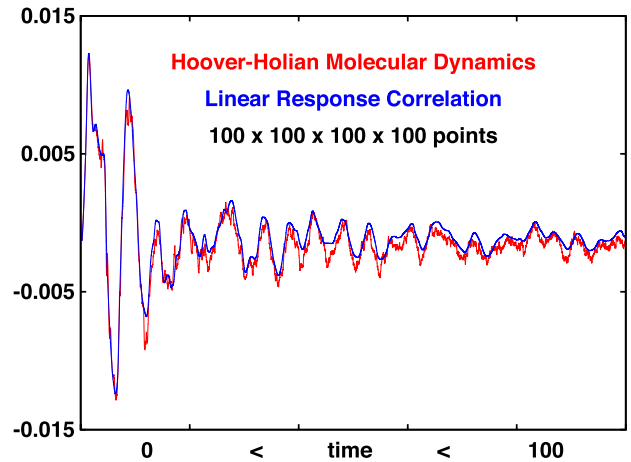


Fig. 4. Comparison of the linear-response correlation integral (in blue) with the measured current (red) for the HH oscillator at a field strength  $\epsilon = 0.10$ . Numerical results for  $T = 1 + 0.10 \tanh(q)$  (shown here) and  $T = [1 - 0.10 \tanh(q)]^{-1}$  are very similar and confirm that  $\epsilon = 0.10$  is close to the linear regime. The phase-space integration uses  $100^4$  equally-probable Gaussian points as the initial states for the averaged current  $\langle p^3/2 \rangle$  and for the linear-response correlation integral.

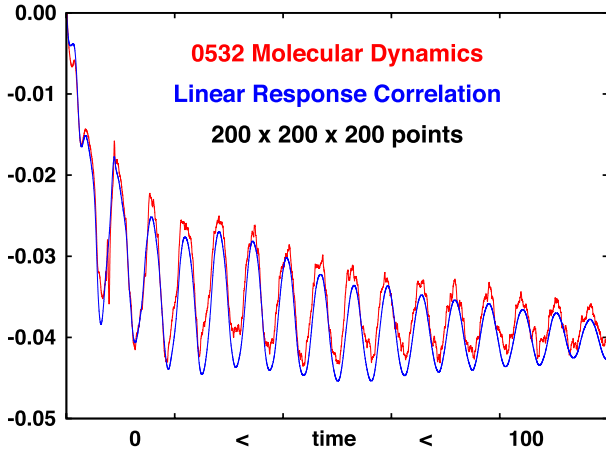


Fig. 5. Comparison of the linear-response correlation integral with the measured current for the 0532 oscillator at a field strength  $\epsilon = 0.10$ . We show results for  $T = 1 + 0.10 \tanh(q)$  which closely resemble those for  $T = [1 - 0.10 \tanh(q)]^{-1}$  confirming that  $\epsilon = 0.10$  is close to the linear regime. The three-dimensional Gaussian phase-space integration uses  $200^3$  equally-probable points as the initial states for both the average current and the correlation integral.

### 5.2. 0532 Model oscillator with temperature gradient

The 0532 Model has only three phase-space dimensions rather than four so that the linear response simulation is about three orders of magnitude, one thousand times, faster. The agreement between the linear-response and directly measured current is likewise excellent, as is shown in Fig. 5. Evidently the ergodic thermostats reproduce both Gibbs' canonical distribution and linear nonequilibrium perturbations as described by Green-Kubo theory.

## 6. Summary and Historical Perspective

A wide variety of time-reversible thermostats all generate Gibbs' canonical ensemble through deterministic chaos. When the kinetic temperature varies with coordinate, the resulting heat current ( $p^3/2$ ) leads to dissipation, heat transfer, and entropy change. The steady loss of comoving phase volume obeys Gibbs' thermodynamic relations in the extended phase space:

$$\left\langle \left( \frac{\dot{S}}{k} \right) = \left( \frac{\dot{Q}}{kT} \right) = \left( \frac{\dot{\otimes}}{\otimes} \right) \right\rangle,$$

where the comoving phase volume includes extensions in the thermostat directions. These time-averaged relations hold even for the nonergodic

Nosé-Hoover oscillator:

$$\begin{aligned} \left\langle \left( \frac{\dot{\otimes}}{\otimes} \right) \right\rangle &= -\langle \zeta \rangle = -\left\langle \zeta \left( \frac{p^2}{T} \right) \right\rangle \\ &= \left\langle \left( \frac{\dot{S}}{k} \right) \right\rangle \quad [\text{NH}]. \end{aligned}$$

Because the ergodic thermostats all generate Gibbs' canonical distribution, they also give linear-response relations linking the nonequilibrium currents and thermal gradients. We believe that these observations are fundamental to a systematic exploration of nonequilibrium statistical mechanics through thermostated dynamics.

Our present day understanding of nonequilibrium systems has its basis in the work of Boltzmann, the Ehrenfests, Gibbs, Maxwell, and Nosé. Fifty years of numerical work have provided alternatives to their classic Hamiltonian and stochastic models. Deterministic reproducibility with dissipative time-reversibility have provided explicit links between microscopic nonequilibrium molecular dynamics and macroscopic thermodynamics.

Shockwave studies which generate localized far-from-equilibrium states would seem to be an ideal problem for consolidating these gains in understanding. Shock dynamics is purely Hamiltonian inside the wave and with equilibrium cold and hot boundaries. The relaxation times correspond to vibrational collision times. The nonlinear dependence of transport coefficients and the irreversible nature of the timelag between forces and fluxes can be measured directly in shockwaves [Hoover *et al.*, 2010]. There is a comprehensive listing of nearly all the existing approaches to nonequilibrium systems in Jepps and Rondoni's review article [Jepps & Rondoni, 2010]. This variety illustrates that many tools for the exploration of these problems are close at hand. The only thing lacking in the shockwave problems is a simple model example like the Galton Board [Hoover *et al.*, 2015b] and the conducting oscillator studied here.

### Acknowledgment

We thank John Ramshaw (Lawrence Livermore National Laboratory) for a continuing series of thought-provoking emails and for sharing his recent work describing the canonical thermostating of dynamical systems in very general terms [Ramshaw, 2015].

## References

- Bulgac, A. & Kusnezov, D. [1990] "Canonical ensemble averages from pseudomicrocanonical dynamics," *Phys. Rev. A* **42**, 5045–5048.
- Cohen, E. G. D. & Rondoni, L. [1998] "Note on phase-space contraction and entropy production in thermostated Hamiltonian systems," *Chaos* **8**, 357–365.
- Daems, D. & Nicolis, G. [1999] "Entropy production and phase-space volume contraction," *Phys. Rev. E* **59**, 4000–4006.
- Hoover, W. G. [1985] "Canonical dynamics: Equilibrium phase-space distributions," *Phys. Rev. A* **31**, 1695–1697.
- Hoover, W. G. & Holian, B. L. [1996] "Kinetic moments method for the canonical ensemble distribution," *Phys. Lett. A* **211**, 253–257.
- Hoover, W. G. [1997] "Mécanique de non-équilibre à la californienne," *Physica A* **240**, 1–11.
- Hoover, W. G., Hoover, C. G. & Uribe, F. J. [2010] "Flexible macroscopic models for dense-fluid shockwaves: Partitioning heat and work; delaying stress and heat flux; two-temperature thermal relaxation," *Proc. Advanced Problems in Mechanics* (1–5 July 2010), sponsored by the Institute for Problems in Mechanical Engineering under the patronage of the Russian Academy of Sciences, arXiv:1005.1525.
- Hoover, W. G. & Hoover, C. G. [2015] "Comparison of very smooth cell-model trajectories using five symplectic and two Runge–Kutta integrators," *Commun. Sci. Technol.* **23**, 109–116.
- Hoover, W. G., Sprott, J. C. & Patra, P. K. [2015a] "Deterministic time-reversible thermostats: Chaos, ergodicity, and the zeroth law of thermodynamics," *Molec. Phys.* **113**, 2863–2872.
- Hoover, W. G., Hoover, C. G. & Sprott, J. C. [2015b] "Hard disks and harmonic oscillators near and far from equilibrium," *Molec. Simul.*, in press.
- Hoover, W. G., Sprott, J. C. & Patra, P. K. [2015c] "Ergodic time-reversible chaos for Gibbs' canonical oscillator," *Phys. Lett. A* **379**, 2935–2940.
- Hoover, W. G., Sprott, J. C. & Hoover, C. G. [2016] "Ergodicity of a singly-thermostated harmonic oscillator," *Commun. Nonlin. Sci. Numer. Simul.* **32**, 234–240.
- Jepps, O. G. & Rondoni, L. [2010] "Deterministic thermostats, theories of nonequilibrium systems and parallels with the ergodic condition," *J. Phys.* **43**, 1–42.
- Ju, N. & Bulgac, A. [1993] "Finite-temperature properties of sodium clusters," *Phys. Rev. B* **48**, 2721–2732.
- Kusnezov, D., Bulgac, A. & Bauer, W. [1990] "Canonical ensembles from chaos," *Ann. Phys.* **204**, 155–185.
- Kusnezov, D. & Bulgac, A. [1992] "Canonical ensembles from chaos II: Constrained dynamical systems," *Ann. Phys.* **214**, 180–218.
- Martyna, G. J., Klein, M. L. & Tuckerman, M. [1992] "Nosé–Hoover chains: The canonical ensemble via continuous dynamics," *J. Chem. Phys.* **97**, 2635–2643.
- Nosé, S. [1984a] "A molecular dynamics method for simulations in the canonical ensemble," *Molec. Phys.* **52**, 255–268.
- Nosé, S. [1984b] "A unified formulation of the constant temperature molecular dynamics methods," *J. Chem. Phys.* **81**, 511–519.
- Ramshaw, J. D. [2015] "A general formalism for singly-thermostated Hamiltonian dynamics," *Phys. Rev. E* **92**, 052138.
- van Beijeren, H. & Dorfman, J. R. [2000] "On thermostats and entropy production," *Physica A* **279**, 21–29.